DOI: https://doi.org/10.68732/d7848247b5c37ca4

ISBN: 978-9989-2053-6-1

Damage characteristics of thermally treated sandstone using the block punch index test

Sourav Das, Ratan Das & Debasish Mazumder
Rock Mechanics and Rock Engineering Laboratory, Department of Geology,
Cotton University, Guwahati, Assam 781001, India
gly2391001_sourav@cottonuniversity.ac.in
0000-0002-9623-9408

Abstract

The strength characteristics of rock represent an important parameter in geotechnical and engineering applications. While the uniaxial compressive strength (UCS) test is widely utilized, it requires extensive sample preparation and difficulties in evaluating the strength properties of weak, foliated rocks. As an alternative, the Block Punch Index (BPI) test is suitable for thinly bedded rocks; however, the effect of BPI on thermally treated rock remained unexplored.

This research investigates BPI strength variations on calcareous sandstone that have been heated under the range of temperatures upto 800° C, maintained in a muffle furnace for 6 hours, and then cooled to room temperature. The results indicated that with the increase in temperature, the BPI value of the rock decreases, from 15.13 MPa at 25°C to 5.75 MPa at 800 °C. A maximum BPI strength around 22.21 MPa was recorded for the sample treated at 500 °C, as grain expansion fills pores and fissures, making the rock denser and thereby increasing the strength of the specimen. Beyond that, the strength reduction continued till 800° C due to the development of microcracks, as confirmed with linear crack density analysis of the microphotographs. The mechanical degradation of the rock exhibited a non-linear pattern across the entire temperature range tested. Moreover, the porosity of the specimen has increased from 3.16% (room temperature) to 11.76% at 800 °C. In addition, color transitions from grey to rust red were observed, due to iron oxidation. Furthermore, an endothermic peak was observed around ~760-780 °C, which must be due to the decomposition of $CaCO_3$ into CaO.

These findings will provide essential information on the physico-mechanical properties of sandstone, with practical implications for engineering applications such as geothermal energy extraction, nuclear waste disposal, and underground coal gasification.

Keywords

Block punch index test, Thermal treatment, Sandstone, Strength degradation.

1 Introduction

The study of thermal alterations to the physico-mechanical properties of rocks is important in various engineering fields, such as geothermal energy extraction, underground coal gasification (UCG), and nuclear waste disposal (Sirdesai et al. 2017). The study of the physico-mechanical properties of hot dry rock (HDR) is one of the important types of research in the process of geothermal energy development (Li et al. 2024). Therefore, it is important to understand the behavior of rock after thermal treatment. Geothermal energy is a sustainable, clean, and stable energy source that does not affect air quality and, therefore, serves as an alternative source to fossil energy (Xie et al. 2020; Feng et al. 2020; Long et al. 2021). Geothermal energy within the first 10 km of Earth's upper crust is about 1.3 x 10^{27} J, and this could supply global energy for approximately 217 million years (Lu 2018). Han et al. (2019) studied the effects of rapid thermal cycling (RTC) on the physical and mechanical properties of sandstone subjected to temperatures ranging from 100˚C to 800˚C. The results indicate that as temperature increases, both the P-wave velocity and sandstone density decrease, with the P-wave velocity showing a greater reduction than density. Additionally, the uniaxial compressive strength and elastic modulus of sandstone were observed to change in a similar pattern with increasing temperature after RTC treatments.

The generation of heat flux from high-level nuclear waste for an extended period increases the temperature of the surrounding rock. Gautam et al. (2019) investigated the thermal properties of Jalore granite for nuclear waste repository using the transient plane source technique. The result indicated that thermal conductivity, thermal diffusivity, mass loss, and elastic wave velocity of Jalore granite decrease gradually as the temperature increases from 25-250 °C.Hu et al. (2022) studied the effects of thermal shock fatigue on the physico-mechanical properties of limestone. The results show that the p-wave velocity, thermal conductivity, and tensile strength of limestone decrease with increasing temperature at a constant number of thermal cycles. Zhang et al. (2026) developed a new multidimensional rock integrity coefficient system to investigate the potential granite host site for a repository in China. The result tracked over a 100-year period, revealing a progressive degradation of integrity parameters under decaying thermal load, with identifiable inflection points at 10 and 40 years.

The gasification of coal, under site conditions, is conducted at temperatures above 700˚C. The temperature in the cavity may reach temperatures as high as 1500˚C (Sirdesai et al. 2015). Deng et al. (2022) found the influence of the cooling rate on the physical and chemical properties of granite heated at 25-800˚C. It is found that water-cooled specimens exhibit more acoustic emission (AE) signals and larger cracks than natural-cooled specimens, as confirmed by the b-value method. Polarized light microscopy reveals higher crack density and connectivity under water cooling. X-ray diffraction (XRD) analysis shows no significant changes in mineral content or diffraction angle, indicating that mechanical property changes are unrelated to chemical properties. Akdag et al. (2023) investigated the dynamic Mode I fracture toughness tests using a split Hopkinson pressure bar (SHPB) on Cracked Chevron Notched Semicircular Bend (CCNSCB) granite specimens. The results showed that fracture initiation toughness and energy distribution are strongly influenced by loading rate and temperature. Higher loading rates changed the failure modes from axial splitting to pulverization.

Many researchers have utilized different mechanical analyses to evaluate the strength of thermally treated specimens, with Uniaxial compressive strength (UCS) test being the most used approach. However, the UCS test requires extensive specimen preparation, which is difficult for thinly bedded, foliated rocks or those containing fossil fragments. In such cases, obtaining a recommended standard-size specimen becomes challenging. As an alternative, the block punch index (BPI) test provides a practical and efficient method for strength analysis of rocks. Moreover, the studies investigating the behavior of thermally treated specimens using the BPI test remain limited. Hence, this research will fulfill the knowledge gap by examining the mechanical strength of thermally treated calcareous sandstone with the BPI test, along with linear crack density, porosity, and DSC analysis.

2 Materials and methods

Field and laboratory investigations were conducted to attain the research objectives. The present research is illustrated in the methodology flow chart in Fig. 1.

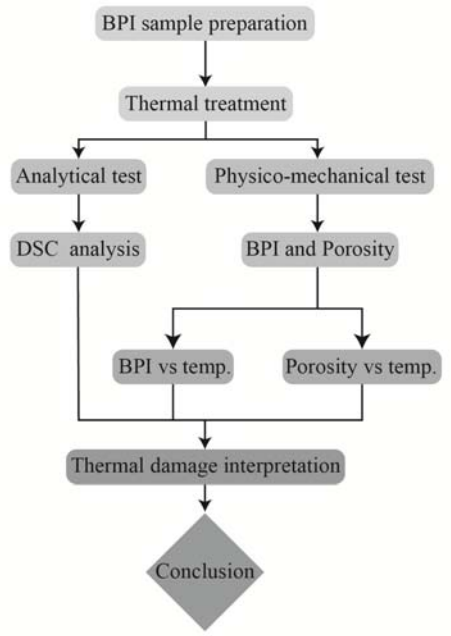


Fig. 1 Methodology flow chart.

2.1 Field visit and sample preparation

Field-collected sandstone samples(from NH-207, Dawki road (22°13′37.11″ N 91°57′44.85″ E) within the East Khasi Hills district of Meghalaya, Northeast India, near Sohlong village (Fig. 2)), have been processed in the laboratory to obtain BPI samples of uniform dimensions for thermal and physico-mechanical testing.

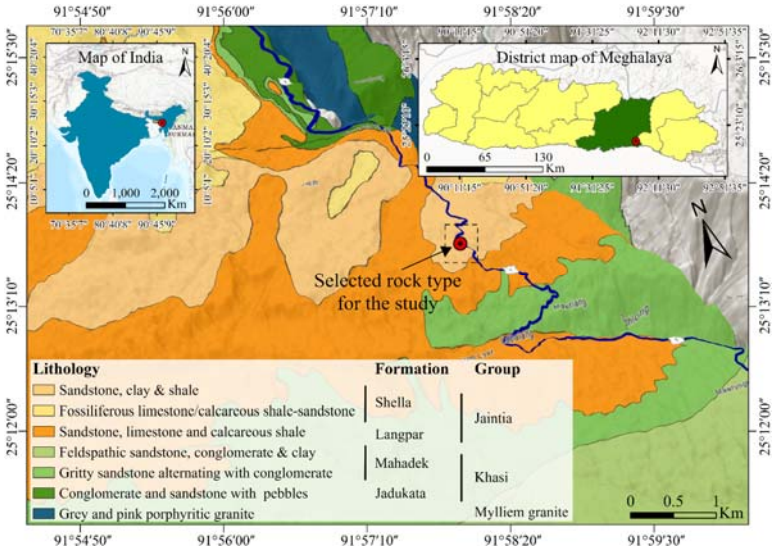


Fig. 2 Map showing the collected source rock lithology (Bhukosh 2025).

2.2 Heat treatment

Calcareous sandstone specimens were utilized to examine the thermal effects on their physico-mechanical properties. Nine specific temperature levels were set: 25° C, 100° C, 200° C, 300° C, 400° C, 500° C, 600° C, 700° C, and 800° C. Two specimens at each temperature were used to investigate the effect of heating on the mechanical properties of sandstone. The thermal treatment was conducted utilizing a muffle furnace (max temperature 1200°C), with a heating rate of 10 °C/min. The specimens were held at a set temperature for 6 hours in the furnace to ensure a consistent temperature distribution across all specimens, and then cooled down to room temperature by the thermal inertia of the furnace (average cooling rate ~4.5°C).

2.2.1 Analytical test

Detailed petrographic studies were conducted using an optical microscope (Leica DM2700 P) to analyze the linear crack density (LCD) of the specimen. Along with petrographic analysis, DSC (NETZSCH STA 449F3) was also utilized to understand the various chemical changes that occurred

due to exposure to high temperatures. The test was carried out at the sophisticated analytical instrument facility (SAIF), IIT Guwahati, India. In this analysis, 13.4 mg sample was heated from room temperature to 1200° C at a constant rate of 10°C/min and has been performed in an inert environment.

2.2.2 Mechanical test

The mechanical behavior of the thermally treated sandstone specimens was evaluated using the BPI test, recommended by Ulusay et al. (2001). The BPI test equipment, along with test specimens, has been shown in Fig. 3.

The uncorrected block punch strength index BPI (in MPa) is calculated from the following equation:

$$BPI = \frac{10^{-3} F_{t,D}}{A} \quad (1)$$

where $F_{t,D}$ is the failure load recorded from the gauge in kN (and converted to MN by the multiplication of 10^{-3}), and A is the area (in m^2) through which the shearing takes place. The formula quoted below is for the area

$$A = 4t(r^2 - 95.1)^{0.5} \times 10^{-6} (m^2) \quad (2)$$

where t and r are the thickness and radius of a disc specimen (in mm), respectively

For each temperature condition, multiple specimens were tested, and the average BPI value was determined to understand the mechanical behavior of the thermally treated calcareous sandstone.

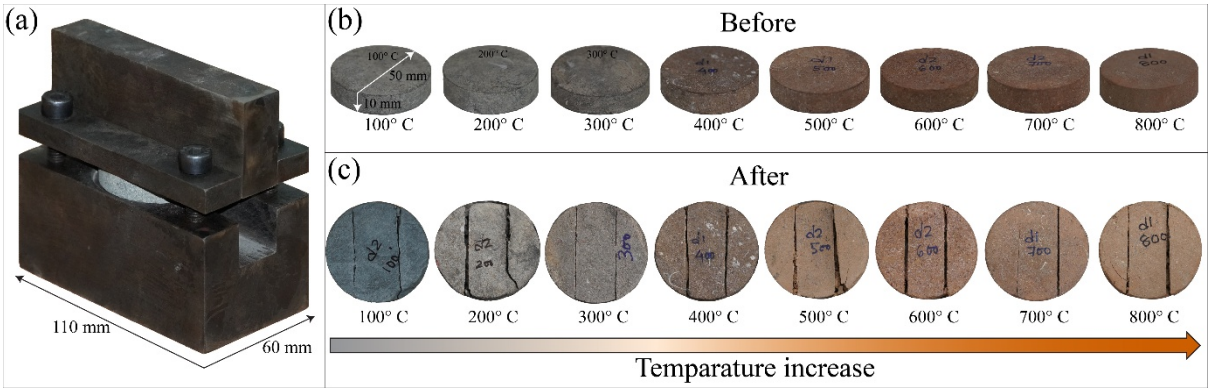


Fig. 3 (a) Block punch index test equipment, (b) and (c) Before and after images of thermally treated specimens.

3 Results and discussion

3.1 Variation of linear crack density in thin sections after thermal treatment

Skeleton analysis in *ImageJ* was used to extract the number of branches and the average branch length of cracks on thermally treated thin sections of calcareous sandstone specimens (Fig. 4). The length of each crack was estimated as the product of the branch number and the average branch length. The total crack length was obtained by totalling the lengths of all cracks. The length of each crack was estimated as the product of the number of branches and the average branch length obtained from Image J.

$$L = N_b \times L_b \quad (1)$$

Where N_b = number of branches of a crack

L_b= average branch length

The total crack length of the microphotograph was then obtained by summing the lengths of all the identified cracks. The linear crack density was defined as the ratio of total crack length to the surface area of the specimen

$$\rho_l = \frac{L_{total}}{A} \quad (2)$$

Where, ρ_l is the linear crack density (mm^{-1}) and

A is the surface area of the specimen (mm^2)

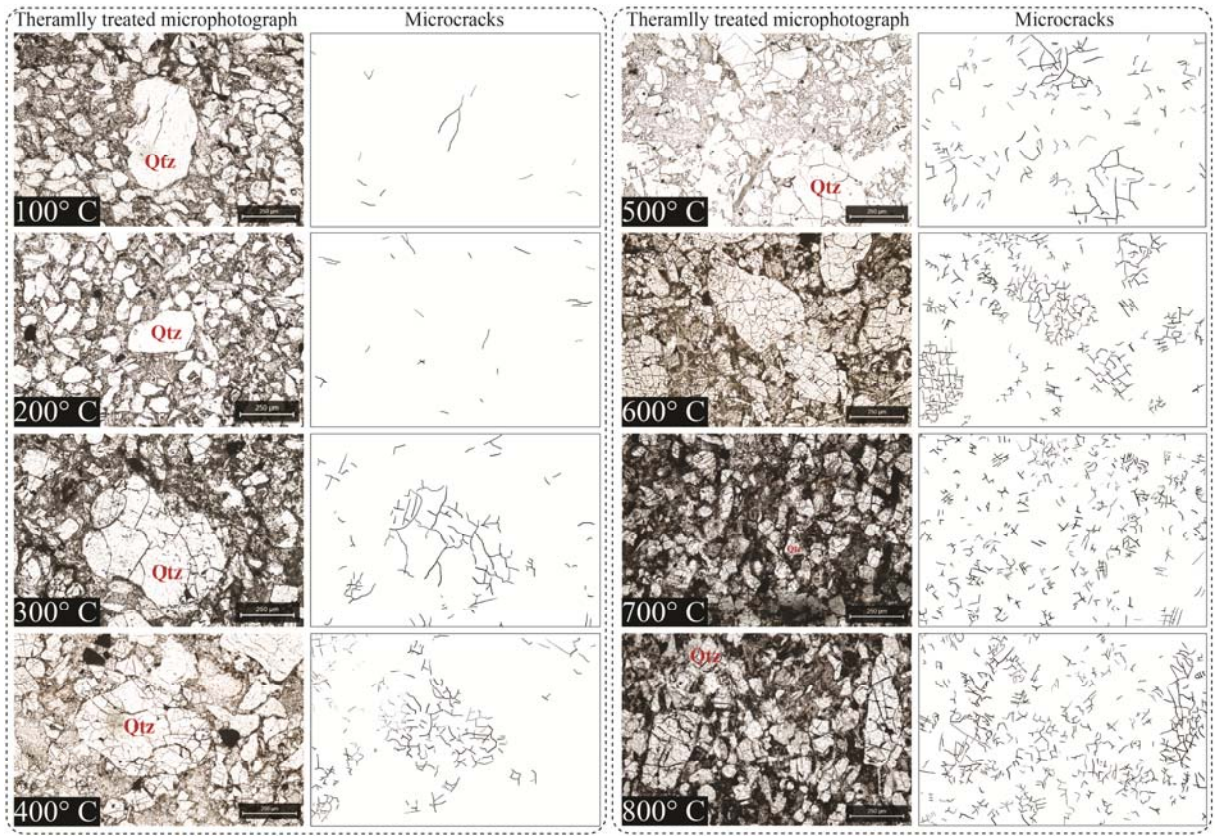


Fig. 4 Variation of microcracks on thermally treated calcareous sandstone microphotographs.

At 100-200 °C, the increase in LCD was less(3.61 mm^{-1} to 4.93 mm^{-1}) (Fig. 5a), due to the evaporation of pore water and the initial thermal expansion of mineral grains.An increase in LCD was observed between 300 °C and 400 °C, where LCD rises to 12.00 mm^{-1} (~3.32 times increase in crack density when compared to 100° C specimen), suggesting enhanced crack initiation and propagation due to differential thermal expansion between quartz grains and surrounding cement.However, beyond 600 °C, the LCD increases sharply, 23.63 mm^{-1} at 800 °C, which is almost 6.54 times the increase in crack density compared to the 100 °C specimen, indicating severe thermal damage and extensive microcrack development caused by high temperature. The linear regression trend ($y = 0.02x + 0.46$; $R^2 = 0.90$) confirms a relationship between temperature and crack density, indicating that an increase in temperature increases microcracks in calcareous sandstone.

3.2 DSC analysis

The DSC analysis has been divided into three temperature ranges. In Stage I, the DSC curve shows an endothermic peak near ~200°C, corresponding to the evaporation of water (free water, adhered water, bound water, and structural water). At~300 °C (Fig. 5b), reduction in heat flow was observed, which is due to the decomposition of amorphous carbonate minerals (Igami et al. 2025) and pre-dihydroxylation of clay minerals(Balek and Murat 1996). Beyond ~300 °C which is stage II, the DSC increases, reaching ~3.7-3.8 mW mg^{-1} near 650-700°C.The enhanced heat absorption by the specimen is due to the differential expansion of mineral grains and the α-β quartz transition at ~573 °C. This transition involves volumetric expansion that generates grain-scale stress, which can induce microcracking in quartz-bearing rock (Johnson et al. 2021). A decrease in heat flow around ~760-780 °C was observed, which may be due to decomposition of $CaCO_3$ ($CaCO_3 \rightarrow CaO + CO_2$).Studies by Igami et al. (2025) also confirms that, peak around 700-800 is attributed to the decomposition of calcite. Furthermore, beyond ~800 °C (Stage III), the decline in DSC intensity indicates the completion of carbonate decomposition, as calcite transforms into CaO with the disappearance of the calcite at high temperatures (Karunadasa et al. 2019).

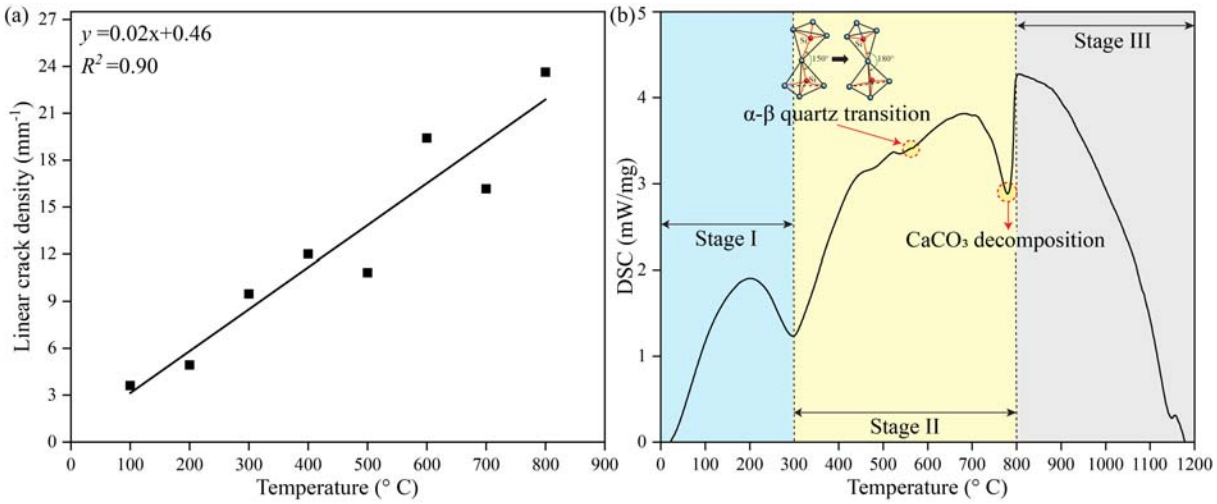


Fig. 5 (a) shows the variation in linear crack density (LCD) of thermally treated thin-section microphotographs of calcareous sandstone specimens, and (b) DSC analyses of calcareous sandstone specimen.

3.3 BPItest analysis

Before the BPI test, a distinct colour transition from grey to rust red was observed on the thermally treated calcareous sandstone, due to iron oxidation (Fig. 3b). The change in colour is a macroscopic indicator of mineralogical and chemical alteration, which may indirectly reflect the thermal damage to the specimen as temperatures increase. Fig. 6 shows the variation of porosity and BPIof calcareous sandstone with temperature.At 25-300° C, the BPI decreases from ~15.13 MPa to ~9.45 MPa (37.5% decrease in strength). It is due to the evaporation of pore-bound water and the formation of initial microcracks.Sirdesai et al. (2017)has also observed a reduction in strength at low temperatures, due to the evaporation of free water from inherent microcracks. However, an increase in strengthwas observed at 500 °C (22.2 MPa), as grain expansion fills pores. Beyond 500 °C, a sharp decline in strength has been observed, decreasing to 14.5 MPa at 600 °C, 10.6 MPa at 700 °C, and ultimately reaching about 5.8 MPa at 800 °C which is overall 61.99% decrease in strength when compared to the room temperature specimen. The strength reduction corresponds to continuous expansion, phase transition of the minerals, and carbonate decomposition at higher temperatures, which leads to the generation of intergranular and intragranular cracks in the specimen. As the grain disintegrates, it loses cohesion, and thus, thermal damage increases with increasing temperature.At lower temperatures (25-300 °C), the BPI decreases from approximately 15.1 MPa to about 9.4 MPa, while porosity shows minor fluctuations (around 3-4%). As the temperature increases to 400-500 °C, the BPI increases, reaching a peak of approximately 22.2 MPa at 500 °C, while porosity remains relatively moderate (4-6%). The temporary increase in strength is due tothe thermal expansion of mineral grains. The volumetricincrease in grain tightens the grains framework, thereby increasingthe strength of the rock(Dong et al. 2022).However, beyond 500 °C, the mechanical behavior changes as porosity increases sharply from approximately 6.8 % at 600 °C to nearly 11-12 % at 800 °C, while the BPI correspondingly decreases from 14.5 MPa to about 5.8 MPa. The increase in porosity is caused by the generation of new microcracks, grain boundary separation, and mineralogical transformations (~573 °C), as well as the decomposition of carbonate cement at higher temperatures. Similar to the present results, in the study of Den'gina et al. (1993) it was observed that at high temperatures, the grains show thermal expansion which leads to the formation of microcracks and subsequently leads to change in porosity. These processes disturb the internal bonding between mineral grains, which leads to formation of interconnected pore networks. Overall, the observed trend indicates that increasing porosity due to thermal damage plays a dominant role in controlling the mechanical deterioration of the sandstone, leading to a significant decline in BPI strength at higher temperatures.

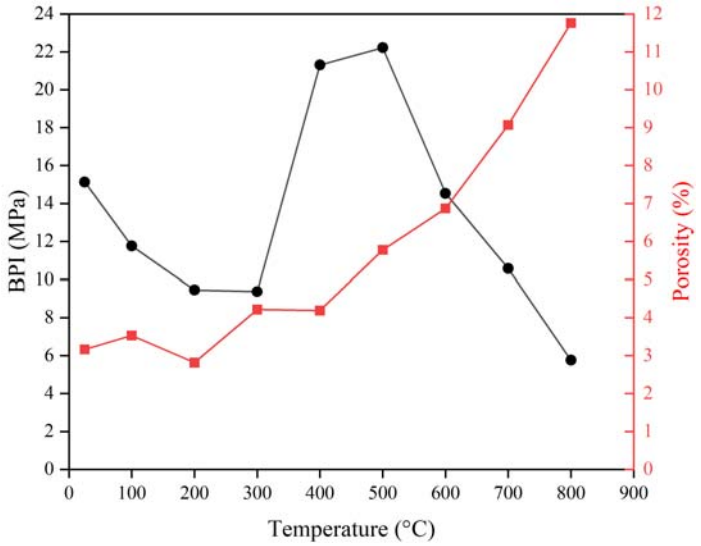


Fig. 6 Variation of BPI and porosity with increasing temperature.

4 Conclusion

- At 100-200 °C, the increase in LCD was less (3.61 mm^{-1} to 4.93 mm^{-1}), due to the evaporation of pore water and the initial thermal expansion of mineral grains. However, beyond 600 °C, the LCD increases sharply at 800 °C (6.54 times increase in crack density compared to the 100 °C specimen), indicating severe thermal damage and extensive microcrack development at high temperature.
- DSC analysis identified dehydration, α-β quartz transition, and calcite decomposition of calcareous sandstone
- A distinct color transition from grey to rust red was observed on the thermally treated calcareous sandstone, due to iron oxidation. Moreover, at 25-300° C, the BPI decreases from ~15.13 MPa to ~9.45 MPa (37.5% decrease in strength), whereas 61.99% decrease in strength was observed at 800° C when compared to the room temperature specimen.
- Overall, these findings will provide essential information about the physico-mechanical properties of sandstone, which has practical implications for engineering applications such as geothermal energy extraction, nuclear waste disposal, and underground coal gasification projects.

Author Contributions

Sourav Das: Writing - original draft, Fieldwork, Software, Data preparation & processing, Formal analysis. **Ratan Das:** Conceptualization, Supervision, Writing - review & editing, Funding acquisition, Resources, Formal analysis, Validation. **Debasish Mazumder**: Fieldwork, Formal analysis.

Funding

No funding was received for the preparation of this manuscript.

Data availability The dataset is included in the manuscript.

Declarations

Conflict of interest

The authors declare that they have no known competing financial interests or personal relationships that could have appeared to influence the work reported in this paper.

Acknowledgement
The research was conducted at the Rock Mechanics and Rock Engineering Laboratory in the Department of Geology at Cotton University, Guwahati, Assam, India. Laboratory testing of rocks was partly supported by the Anusandhan National Research Foundation (formerly known as Science and Engineering Research Board), Government of India, under the start-up Research Grant (SRG) scheme (File Number: ANRF, SRG/2022/000447) funded to RD

References

Akdag S, Karakus M, Nguyen GD, et al (2023) Dynamic response and fracture characteristics of thermally-treated granite under dynamic loading. Int J Rock Mech Min Sci 170:105482. https://doi.org/10.1016/j.ijrmms.2023.105482

Balek V, Murat M (1996) The emanation thermal analysis of kaolinite clay minerals. Thermochim Acta 282–283:385–397. https://doi.org/10.1016/0040-6031(96)02886-9

Bhukosh (2025) Geological Survey of India, Bhukosh. In: Gov. India, Kolkata, India. https://bhukosh.gsi.gov.in/. Accessed 8 Sep 2025

Den'gina NI, Kazak VN, Pristash V V. (1993) Changes in rocks at high temperatures. J Min Sci 29:472–477. https://doi.org/10.1007/BF00733026

Deng L, Li X, Wu Y, et al (2022) Influence of cooling speed on the physical and mechanical properties of granite in geothermal-related engineering. Deep Undergr Sci Eng 1:40–57. https://doi.org/10.1002/dug2.12011

Dong Z, Chen Y, Wang X, et al (2022) Evaluation of Thermophysical and Mechanical Properties of Sandstone Due to High-Temperature. Materials (Basel) 15:8692. https://doi.org/10.3390/ma15238692

Feng G, Wang X, Wang M, Kang Y (2020) Experimental investigation of thermal cycling effect on fracture characteristics of granite in a geothermal-energy reservoir. Eng Fract Mech 235:107180. https://doi.org/10.1016/j.engfracmech.2020.107180

Gautam PK, Verma AK, Singh TN, et al (2019) Experimental investigations on the thermal properties of Jalore granitic rocks for nuclear waste repository. Thermochim Acta 681:178381. https://doi.org/10.1016/j.tca.2019.178381

Han G, Jing H, Su H, et al (2019) Effects of thermal shock due to rapid cooling on the mechanical properties of sandstone. Environ Earth Sci 78:146. https://doi.org/10.1007/s12665-019-8151-1

Hu J, Xie H, Gao M, et al (2022) Damage mechanism and heat transfer characteristics of limestone after thermal shock cycle treatments based on geothermal development. Int J Rock Mech Min Sci 160:105269. https://doi.org/10.1016/j.ijrmms.2022.105269

Igami R, Igarashi G, Aili A, et al (2025) Clinker mineral formation and thermal decomposition of calcium carbonates in carbonated tobermorites: Mechanism of CO2 release in low-temperature ranges. Cem Concr Res 197:107969. https://doi.org/10.1016/j.cemconres.2025.107969

Johnson SE, Song WJ, Cook AC, et al (2021) The quartz α↔β phase transition: Does it drive damage and reaction in continental crust? Earth Planet Sci Lett 553:116622. https://doi.org/10.1016/j.epsl.2020.116622

Karunadasa KSP, Manoratne CH, Pitawala HMTGA, Rajapakse RMG (2019) Thermal decomposition of calcium carbonate (calcite polymorph) as examined by in-situ high-temperature X-ray powder diffraction. J Phys Chem Solids 134:21–28. https://doi.org/10.1016/j.jpcs.2019.05.023

Li P, Zhang H, Wu Y (2024) Study on the evolution of mechanical properties of hot dry rocks after supercritical CO2 injection. Geotherm Energy 12:27. https://doi.org/10.1186/s40517-024-00306-5

Long X, Xie H, Deng X, et al (2021) Geological and Geochemical Characteristics of the Geothermal Resources in Rucheng, China. Lithosphere 2021:. https://doi.org/10.2113/2021/1357568

Lu S-M (2018) A global review of enhanced geothermal system (EGS). Renew Sustain Energy Rev 81:2902–2921. https://doi.org/10.1016/j.rser.2017.06.097

Sirdesai NN, Singh R, Singh TN, Ranjith PG (2015) Numerical and experimental study of strata behavior and land subsidence in an underground coal gasification project. Proc Int Assoc Hydrol Sci 372:455–462. https://doi.org/10.5194/piahs-372-455-2015

Sirdesai NN, Singh TN, Pathegama Gamage R (2017) Thermal alterations in the poro-mechanical characteristic of an Indian sandstone – A comparative study. Eng Geol 226:208–220. https://doi.org/10.1016/j.enggeo.2017.06.010

Ulusay R, Gokceoglu C, Sulukcu S (2001) Draft ISRM suggested method for determining block punch strength index (BPI). Int J Rock Mech Min Sci 38:1113–1119. https://doi.org/10.1016/S1365-1609(01)00078-8

Xie H, Li C, Zhou T, et al (2020) Conceptualization and evaluation of the exploration and utilization of low/medium-temperature geothermal energy: a case study of the Guangdong-Hong Kong-Macao Greater Bay Area. Geomech Geophys Geo-Energy Geo-Resources 6:18. https://doi.org/10.1007/s40948-019-00140-1

Zhang M, Liao F, Yang Y, et al (2026) Impact of Granite Thermo-Mechanical Coupling on the Long-Term Integrity of Engineered Barriers System (EBS) in HLW Repositories. Arab J Sci Eng. https://doi.org/10.1007/s13369-026-11106-3